Arch Toxicol (2015) 89:621–633
DOI 10.1007/s00204-014-1428-y

ORGAN TOXICITY AND MECHANISMS

# Pathologic and molecular profiling of rapid-onset fibrosis and inflammation induced by multi-walled carbon nanotubes

**Jie Dong · Dale W. Porter · Lori A. Batteli · Michael G. Wolfarth · Diana L. Richardson · Qiang Ma**

Received: 26 September 2014 / Accepted: 26 November 2014 / Published online: 16 December 2014


**Abstract** Multi-walled carbon nanotubes (MWCNT) are new materials with a wide range of industrial and commercial applications. However, their nano-scaled size and fiber-like shape render them respirable and potentially fibrogenic if inhaled into the lungs. To understand MWCNT fibrogenesis, we analyzed the pathologic and molecular aspects of the early phase response to MWCNT in mouse lungs. MWCNT induced rapid and pronounced lesions in the lungs characterized by increased cellularity and formation of fibrotic foci, most notably near where MWCNT deposited, within 14 days post-exposure. Deposition of collagen fibers was markedly increased in the alveolar septa and fibrotic foci, accompanied by elevated expression of fibrotic genes *Col1a1*, *Col1a2*, and *Fn1* at both mRNA and protein levels. Fibrosis was induced rapidly at 40 μg, wherein fibrotic changes were detected on day 1 and reached a maximal intensity on day 7 through day 14. Induction of fibrosis was dose-dependent at the dose range of 5–40 μg, 7 days post-exposure. MWCNT elicited rapid and prominent infiltrations of neutrophils and macrophages alongside fibrosis implicating acute inflammation in the fibrotic response. At the molecular level, MWCNT induced elevated expression of proinflammatory cytokines TNFα, IL1α, IL1β, IL6, and CCL2 in lung tissues as well as the bronchoalveolar lavage fluid, in a dose- and time-dependent manner. MWCNT also increased the expression of fibrogenic growth factors TGF-β1 and PDGF-A in the lungs significantly. These findings underscore the interplay between acute inflammation and the early fibrotic response in the initiation and propagation of pulmonary fibrosis induced by MWCNT.

**Keywords** Nanotoxicity · Lung fibrosis · Inflammation · Cytokine · Growth factor · Animal model

*Disclaimer* The findings and conclusions in this report are those of the authors and do not necessarily represent the views of the National Institute for Occupational Safety and Health.

J. Dong · Q. Ma (✉)
Receptor Biology Laboratory, Toxicology and Molecular Biology Branch, Health Effects Laboratory Division, National Institute for Occupational Safety and Health, Centers for Disease Control and Prevention, 1095 Willowdale Road, Mailstop 3014, Morgantown, WV 26505, USA
e-mail: qam1@cdc.gov

D. W. Porter · L. A. Batteli · M. G. Wolfarth
Pathology and Physiology Research Branch, Health Effects Laboratory Division, National Institute for Occupational Safety and Health, Centers for Disease Control and Prevention, 1095 Willowdale Road, Morgantown, WV 26505, USA

D. L. Richardson
Pathology Core, Health Effects Laboratory Division, National Institute for Occupational Safety and Health, Centers for Disease Control and Prevention, 1095 Willowdale Road, Morgantown, WV 26505, USA

**Abbreviations**

| | |
|---|---|
| BAL | Bronchoalveolar lavage |
| CNT | Carbon nanotubes |
| DM | Dispersion medium |
| *Gapdh* | Glyceraldehyde 3-phosphate dehydrogenase |
| IL | Interleukin |
| LDH | Lactate dehydrogenase |
| MWCNT | Multi-walled carbon nanotubes |
| PBS | Phosphate-buffered saline |
| PDGF | Platelet-derived growth factor |
| SWCNT | Single-walled carbon nanotubes |
| TGF | Transforming growth factor |
| TNF | Tumor necrosis factor |

## Introduction

Pulmonary exposure to respirable fibers and particles potentially causes lung fibrosis, resulting in significant morbidity and disability in certain occupations (Castranova and Vallyathan 2000; Rom 2007). The mechanism by which fibers and particles elicit fibrosis is not well understood at present. The possibility that many new materials being manufactured or introduced into the market may have fibrogenic effects upon inhalation further emphasizes the need for a better understanding of the pathogenesis of substance-induced lung fibrosis (NIOSH 2013).

Carbon nanotubes (CNT) are new, promising nanomaterials that exhibit remarkable potentials for a wide range of industrial and commercial applications (De Volder et al. 2013; Zhang et al. 2013). Single- or multi-walled CNT (SWCNT, MWCNT) are two major forms of CNT, each having a diameter of <100 nm, a high aspect ratio, and unique physicochemical and electro-conductive properties. CNT may have a complex life cycle that includes the commercialization, consumer usage, disposal, and recovery in addition to invention and manufacturing of the materials (NIOSH 2013). It is known that exposure to respirable fibers with high aspect ratios potentially causes fibrosis in the lungs, such as asbestosis induced by inhalation of asbestos fibers (Rom 2007). In this regard, the nano-scaled size and fiber-like shape of CNT have raised health concerns over potential injuries if inhaled into the lungs of exposed workers and consumers (Buzea et al. 2007; Donaldson et al. 2006; Maynard and Kuempel 2005). Certain forms of SWCNT and MWCNT have been shown to exhibit significant fibrogenic and inflammatory activities in vitro and in animals (He et al. 2012, 2011; Porter et al. 2010; Shvedova et al. 2005).

Several recent studies indicate that MWCNT and SWCNT differ in their fate and fibrogenic potential in the lungs due to differences in their size, shape, rigidity, and solubility. The MWCNT tested are fiber-like with a mean diameter of 49 nm and a length of 3.9 μm, while the SWCNT are thread filament-like with a mean diameter of 1–4 nm and a typical length in several hundred nm (Porter et al. 2010; Shvedova et al. 2005). As a result, the MWCNT are more easily dispersed in solutions than the SWCNT. Upon inhalation, the distribution of the lung burden for the MWCNT was predominantly within alveolar and interstitial macrophages with approximately 8 % delivery to the alveolar septa, whereas that of the SWCNT was more within the interstitial space with few being incorporated into alveolar macrophages (Mercer et al. 2011). The MWCNT appeared to have a greater tendency to penetrate cells and membranous structures, induce granulomatous lesions in the lungs, and reach the pleural space and extra-pulmonary organs (Mercer et al. 2010, 2013a, b; Ryman-Rasmussen et al. 2009). On the basis of equal surface area, the MWCNT were estimated to be about 2.5-fold more fibrogenic than the SWCNT; but, on the basis of equal weight, the SWCNT are more fibrogenic than the MWCNT. Nonetheless, the overall fibrotic responses to the MWCNT and SWCNT appeared similar with a time course resembling that of a foreign substance-induced fibrotic response, wherein the pathologic alterations are initiated with an acute phase response followed by chronic interstitial fibrosis with or without the formation of granulomas (Mercer et al. 2013a; Porter et al. 2013, 2010; Shvedova et al. 2005).

Little is known about how CNT trigger and maintain fibrogenesis in the lungs at molecular and cellular levels. The chronic phase fibrosis is generally emphasized in the study of lung fibrosis, because it reflects the stable or progressive fibrotic pathology directly, whereas the acute phase pathology often decreases in intensity considerably within weeks. Consistent with this notion, it has been suggested that CNT stimulate fibroblast proliferation directly and, thereby, induce fibrosis (Mercer et al. 2011), though evidence supporting a direct stimulatory mode of action to account for the fibrogenic effect of CNT in vivo is lacking at the present time. Alternatively, the findings that both SWCNT and MWCNT, as well as many other fibrogenic fibers and particles, such as asbestos and silica, elicit similar and significant acute responses in the lungs prior to chronic fibrosis suggest a role of the early phase response in the initiation and development of induced lung fibrosis. This posit raises two questions with regard to the acute phase response: (a) what it entails in the context of CNT exposure; and (b) how it impacts the fibrotic process in the lungs; in particular, what role, if any, acute inflammation plays in lung fibrogenesis.

To address these questions, we focused the study on systematically examining the pathologic and molecular aspects of the early phase response to MWCNT in mouse lungs. The results reveal that pulmonary exposure to a low dose of MWCNT induced rapid onset of interstitial fibrosis in the lungs evidenced by significantly increased deposition of collagen fibers in the alveolar septa, formation of fibrotic foci, and elevated expression of fibrotic genes. The fibrotic phenotype was detectable as early as day 1 post-exposure, but achieved a climax on day 7 and maintained through day 14. In addition, acute inflammation occurred and was marked with rapid infiltration of neutrophils and macrophages in lung tissues and the bronchoalveolar lavage (BAL) fluid. At the molecular level, MWCNT stimulated rapid production and secretion of multiple proinflammatory and profibrotic cytokines, such as tumor necrosis factor (TNF) α, interleukin (IL) 1α, IL1β, IL6 and CCL2, and growth factors, such as transforming growth factor (TGF)-β1 and platelet-derived growth factor (PDGF)-A, in the lungs. These findings demonstrate a role of the early phase response in MWCNT-induced lung fibrosis

and suggest a mechanistic model in which the cross-talk between acute inflammation and the early fibrogenic response regulates the initiation and propagation of lung fibrosis.

## Materials and methods

### Animal

Eight-week-old male C57BL/6J mice were purchased from Jackson Laboratories (Bar Harbor, ME, USA) and maintained in an accredited, specific pathogen-free, and environmentally controlled facility at National Institute for Occupational Safety and Health. Mice were housed in polycarbonate ventilated cages with HEPA-filtered air and 12-h fluorescent lighting. Mice were maintained on Harlan Teklad Rodent Diet 7913 (Indianapolis, IN, USA) and tap water ad libitum and were monitored for health and specific pathogen-free status regularly. All animal procedures were approved by the local Animal Care and Use Committee of the Institute.

### Carbon nanotubes

MWCNT were obtained from Mitsui & Company (XNRI MWNT-7, lot #05072001K28, Tokyo, Japan) and were fully characterized previously (Porter et al. 2010). Suspensions of MWCNT were prepared freshly in a dispersion medium (DM) containing $Ca^{2+}$- and $Mg^{2+}$-free phosphate-buffered saline (PBS), pH 7.4, supplemented with 0.6 mg/ml mouse serum albumin (Sigma, St. Louis, MO, USA) and 0.01 mg/ml 1,2-dipalmitoyl-sn-glycerol-3-phosphocholine (Sigma) (Porter et al. 2008). DM was used as vehicle control. MWCNT suspensions containing 5, 20, or 40 μg MWCNT in 50 μl DM were used for mouse pharyngeal aspiration.

### Pharyngeal aspiration

Mice were treated with MWCNT by pharyngeal aspiration as described elsewhere (Porter et al. 2010). Isoflurane (Piramal Healthcare, Bethlehem, PA, USA) was used to anesthetize mice. A single dose of 50 μl of DM or MWCNT suspension containing 5, 20, or 40 μg MWCNT was administered following established procedures (Porter et al. 2010). Mouse pharyngeal aspiration has been shown to produce an even distribution of administered materials throughout the lungs (Rao et al. 2003), and aspiration of single-walled CNT elicits similar biological effects to those by inhalation of the CNT (Porter et al. 2013). Thus, pharyngeal aspiration represents a noninvasive and physiologically relevant route of exposure of a specific dose to the lungs in animals.

### Histopathology

Mice were euthanized by intraperitoneal injection of sodium pentobarbital at a dose of >100 mg/kg body weight (Zoetis, Florham Park, NJ, USA). The left lung lobe was removed, fixed with 10 % neutral buffered formalin through intratracheal perfusion, and embedded in paraffin. Sections of 5 μm thickness were subjected to H&E, Masson's trichrome, and Picrosirius red staining following standard procedures. Fibrotic changes were quantified using the modified Ashcroft scale with grades from 0 to 8 as described elsewhere (Hubner et al. 2008).

### Bronchoalveolar lavage

Mice were euthanized with sodium pentobarbital followed by exsanguination. Collection of BAL fluid was performed as described previously (Porter et al. 2010). Briefly, a tracheal cannula was inserted. BAL fluid was obtained through the cannula with ice cold $Ca^{2+}$- and $Mg^{2+}$-free PBS, pH 7.4, supplemented with 5.5 mM D-glucose. The fluid from the first lavage (0.6 ml) was kept on ice. Subsequent lavages, each with 1 ml, were performed and pooled until a total of 4 ml of BAL fluid was collected.

To analyze BAL fluid, cells were isolated by centrifugation at 650×*g* for 5 min at 4 °C. The cell-free supernatant from the first BAL was used for analysis of lactate dehydrogenase (LDH) activity and protein levels of cytokines and growth factors (ELISAs). BAL cells from all BAL fractions from each mouse were pooled after re-suspension in PBS, centrifuged for a second time, and then re-suspended in PBS for further analysis. Total BAL cell counts were determined using a Coulter Multisizer 3 (Coulter Electronics, Hialeah, FL, USA). Cytospin preparations of the BAL cells were performed using a cytocentrifuge (Shandon Elliot Cytocentrifuge, London, GB). The BAL cells on slides from cytospin preparations were stained with modified Wright–Giemsa stain, and cell differentials were determined by light microscopy. The BAL fluid LDH activity, a marker of cytotoxicity, was measured by monitoring the oxidation of lactate to pyruvate (catalyzed by LDH) coupled with the reduction of NAD to NADH at 340 nm using a kit from Roche Diagnostics Systems (Montclair, NJ, USA). BAL fluid LDH activities were assayed using COBAS MIRA Plus Analyzer (Roche Diagnostics Systems, Indianapolis, IN, USA).

### Quantitative real-time PCR

Total RNA was extracted from mouse lungs using RNeasy Mini Kit (QIAGEN, Valencia, CA, USA). One microgram of total RNA was reverse transcribed in a 20 μl reaction with QuantiTect Reverse Transcription system (Qiagen)

to produce cDNA. The reverse transcription products were diluted at 1:10 with nuclease-free water, and 5 μl of diluted cDNA products was used as template for PCR analysis. Real-time PCR was performed using $RT^2$ SYBR Green ROX qPCR Mastermix (Qiagen) with ABI Sequence Detection System 7500 (Applied Biosystems, Grand Island, NY, USA). Mouse housekeeping gene glyceraldehyde 3-phosphate dehydrogenase (*Gapdh*) was used as an internal control for normalization in all PCR reactions. Primer sequences are available upon request. $\Delta C_T$ for each gene was calculated using the $C_T$ values for the gene of interest, and *Gapdh* with the formula $\Delta C_T = C_T^{\text{gene}} - C_T^{Gapdh}$. $\Delta\Delta C_T$ was determined using the formula $\Delta\Delta C_T = \Delta C_T^{\text{treated}} - \Delta C_T^{\text{control}}$. Fold change for each gene was calculated as $2^{(-\Delta\Delta C_T)}$. The fold change values for four samples in each experimental group were averaged and presented as mean ± SD

### Cytokine and growth factor measurements

Protein levels of TNFα, IL6, IL1α, IL1β, and TGF-β1 in BAL fluid were determined using Mouse DuoSet ELISA kits (R&D Systems, Minneapolis, MN, USA). PDGF-AA level in the BAL fluid was quantified using the Human/Mouse PDGF-AA Quantikine ELISA Kit (R&D Systems). An optical density at 450 nm was determined using SPECTRA max 384 PLUS (Molecular Devices, Sunnyvale, CA, USA). Samples from five to six animals per experimental group were measured and calculated as mean ± SD.

### Immunohistochemistry

Formalin-fixed, paraffin-embedded lung tissue sections (left lung lobe, 5 μm) were deparaffinized with three washes of xylene for 5 min each, rehydrated gradually with two washes of 100 % ethanol for 10 min each, two washes of 95 % ethanol for 10 min each, and one wash of 70 % ethanol for 5 min, and then washed twice with deionized water for 5 min each. For antigen unmasking, sections were heated to boil in 10 mM sodium citrate buffer, pH 6.0, and maintained at a sub-boiling temperature for 10 min in a microwave oven. The slides were then cooled on a bench top for 30 min for immunohistochemistry assays.

For immunohistochemistry, slides were incubated with BLOXALL Endogenous Peroxidase and Alkaline Phosphatase Blocking Solution (Vector Laboratories, Burlingame, CA, USA) for 10 min at room temperature to block endogenous peroxidase activity. The assays were performed with the ImmPRESS Polymer Detection system (Vector Laboratories). ImmPACT NovaRED (Vector Laboratories) was applied as the peroxidase substrate (red). Slides were counterstained with Hematoxylin QS (Vector Laboratories), which visualizes nuclei with a blue–violet color. The primary antibodies used for immunohistochemistry included anti-collagen I (Abcam, Cambridge, MA, USA), anti-FN1 (Abcam), anti-Mac-2 (CEDARLANE, Burlington, Ontario, Canada), anti-neutrophil (Abcam), anti-MBP (obtained from the Laboratories of Drs. Nancy A. Lee and James J. Lee, Mayo Clinic, Scottsdale, AZ, USA), anti-mMCP-8 (BioLegend, San Diego, CA, USA), anti-TGF-β1 (Santa Cruz Biotechnology, Inc., Santa Cruz, CA, USA), and anti-PDGF-A (Santa Cruz Biotechnology, Inc.). Images were photographed using Olympus Provis AX-70 system (Olympus, Center Valley, PA, USA). For cell counting, positive cells were counted on five images photographed under 40× magnification from one section of lung tissues; and lung tissues from four mice per experimental group were analyzed. Data were presented as mean ± SD.

### Granulocyte detection

Cells of the granulocytic lineage were determined with the Naphthol AS-D Chloroacetate Esterase kit (Sigma). Formalin-fixed, paraffin-embedded lung tissue sections (left lung lobe, 5 μm) were used. A bright red color indicates sites with high activities of the enzyme from granulocytes in the tissue.

### Statistical analysis

Statistical evaluation of differences between experimental groups was determined by two-tailed Student's *t* test. For comparison of multiple means, one-way ANOVA was performed followed by Tukey's multiple comparison using GraphPad Prism (GraphPad Software, Inc., La Jolla, CA, USA). A $p$ value of <0.05 was considered statistically significant ($^*p < 0.05$; $^{**}p < 0.01$; and $^{***}p < 0.001$).

## Results

### Rapid-onset and pronounced fibrosis in mouse lungs induced by MWCNT

To understand the nature and function of the early phase response in MWCNT-induced lung fibrosis, we first characterized the acute response to pulmonary exposure to single-dose MWCNT. Adult mice were treated with DM (vehicle control) or MWCNT in DM at 40 μg per mouse by pharyngeal aspiration. The lungs were harvested on days 1, 3, 7, and 14 after treatment to recapitulate the time course of the early phase response. As expected, aspiration of DM did not cause notable changes in the respiratory zones of the lungs, but exposure to MWCNT elicited rapid and remarkable alterations in the lungs evidenced

by increased cellularity and clustering of cells and matrix materials in the interstitial space, most notably near the terminal and respiratory bronchioles and alveolar ducts where the nanofibers deposited (Fig. 1a, upper panels). Histological changes were observed as early as day 1 after MWCNT treatment, became progressively more prominent on day 3, and reached a maximal level on day 7. Thereafter, the changes decreased slightly but remained significantly elevated through day 14 as shown by the number and size of the foci.

To examine the fibrotic response directly, we performed Masson's trichrome staining that distinguishes cells from their collagenous connective surroundings and Picrosirius red staining that preferentially detects collagens I and III, two major collagen fibers involved in lung fibrosis (Fig. 1a, lower panels; and data not shown). Elevated accumulation of collagen was observed as early as day 1 post-exposure to MWCNT. Large scale collagen deposition and formation of fibrotic foci became evident on day 3. We quantified the extent of lung fibrosis using a modified Ashcroft score, for

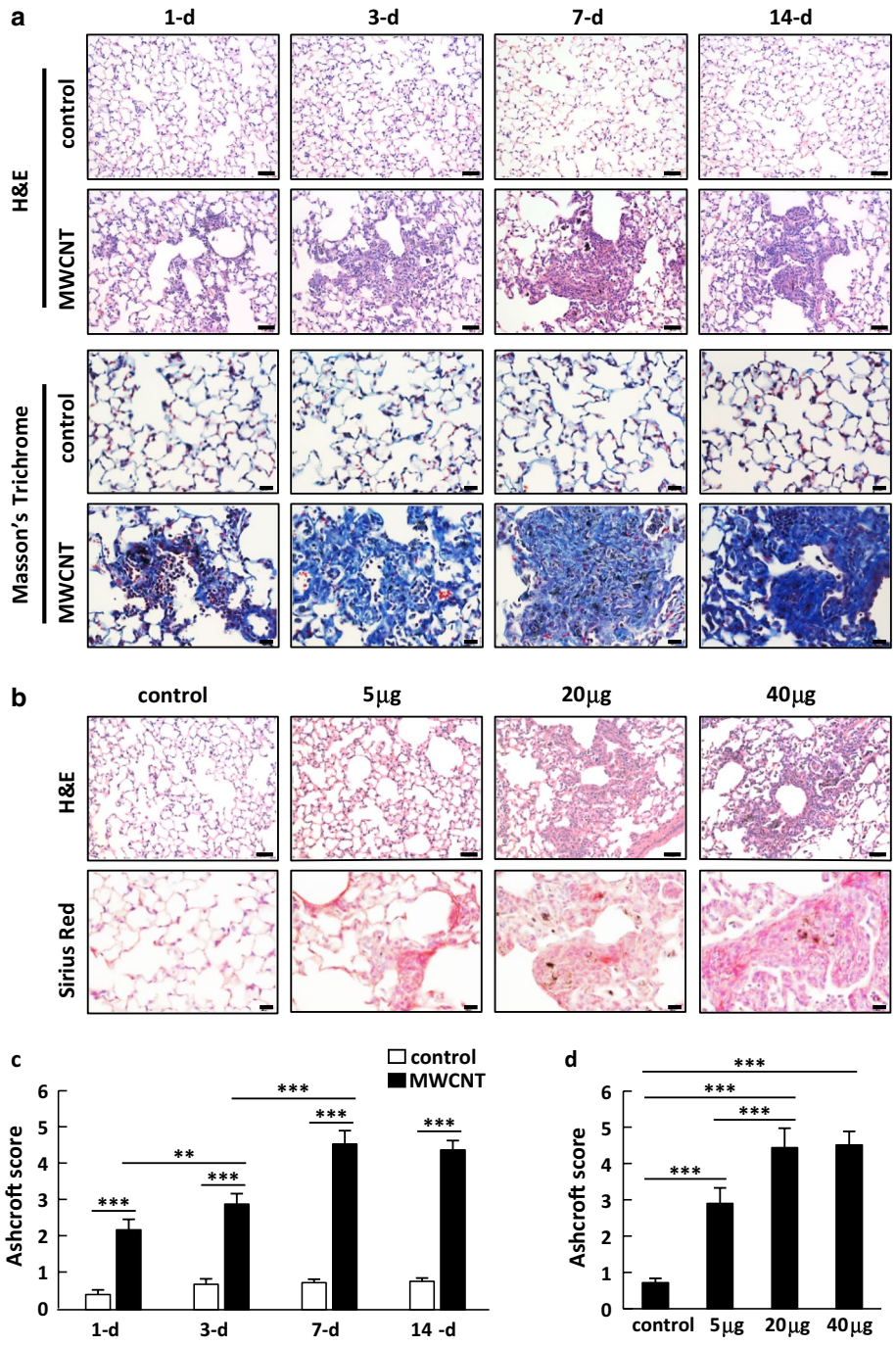


**Fig. 1** Rapid-onset pulmonary fibrosis induced by MWCNT in mice. **a** Time course. Mice received DM or MWCNT (40 μg) and were killed on days 1, 3, 7, and 14 post-exposure. Pathological effects were determined by *H&E* staining (*scale bar* 50 μm), and *collagen fibers* were detected in *blue color* by *Masson's trichrome staining* (*scale bar* 20 μm). **b** Dose dependence. Mice received DM or MWCNT at 5, 20, or 40 μg and were dissected on day 7 post-exposure. Histological alterations were examined by H&E staining (*scale bar* 50 μm), and Picrosirius red staining (*scale bar* 20 μm). *MWCNT* deposits were seen in *black*. Severity of pulmonary fibrosis was evaluated by modified Ashcroft scores represented as mean ± SD ($n = 6$ for each group) for time course, **c** or dose dependence, **d** studies

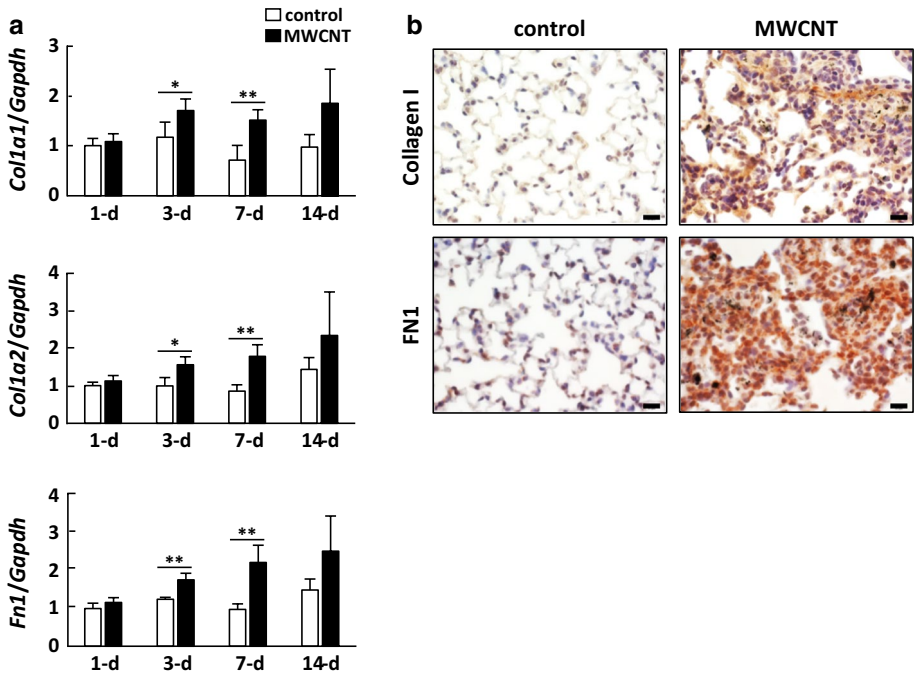


**Fig. 2** Induction of fibrotic marker gene expression. **a** Mice were treated with DM or MWCNT (40 μg). Quantitative PCR analysis was performed, and fold changes of mRNA levels of *Col1a1*, *Col1a2*, and *Fn1* relative to that of *Gapdh* were expressed as mean ± SD ($n = 4$ for each group). **b** Collagen I and FN1 levels were determined by immunohistochemistry on lung sections from mice treated with DM or 40 μg of MWCNT for 7 days. *Red* indicates positive staining, and *blue* indicates nuclear staining (*scale bar* 20 μm). *MWCNT* deposits were shown in *black*

which each successive microscopic field under 20× magnification was given a score to indicate the grade of fibrosis ranging from 0 to 8 that represents from normal lung alveoli without fibrotic burden to complete obliteration of the alveolar space in a fibrotic mass within the microscopic field (Hubner et al. 2008). The Ashcroft scores confirmed that fibrosis occurred on day 1, progressed to a peak level on day 7, and maintained at a similar but slightly reduced level through day 14 (Fig. 1c). The pronounced fibrotic changes were triggered by MWCNT specifically because fibrotic mass formation was not observed in mice treated with DM at all time points examined. These findings reveal pulmonary exposure to MWCNT induces rapid and significant lung fibrosis as a major manifestation of the early phase response.

We performed a dose-dependence study to assess the potency of MWCNT to induce lung fibrosis. Administration of MWCNT at a single dose of 5 μg per mouse led to the development of notable, contiguous fibrotic walls in alveolar septa as well as small-sized fibrotic masses, whereas treatment with a single dose of 20 or 40 μg of MWCNT resulted in the formation of multiple fibrotic foci within 7 days after treatment (Fig. 1b, upper panels). Picrosirius red and Masson's trichrome staining were performed to visualize fibrosis (Fig. 1b, lower panels; and data not shown). A significant increase in the amount of collagen fibers was found in both alveolar septa and fibrotic masses. The Ashcroft score analysis revealed that MWCNT at 5 μg elicited significant lung fibrosis within 7 days after exposure (Fig. 1d). At 20 or 40 μg, MWCNT induced dramatic fibrotic pathology in the lungs. The findings indicate MWCNT trigger lung fibrosis potently at a single low dose.

Lung fibrosis is often marked with elevated expression of fibrotic genes. The effect of MWCNT on the expression of a number of fibrotic marker genes, including *Col1a1* encoding the pro-alpha1 chain of collagen I, *Col1a2* encoding the pro-alpha2 chain of collagen I, and *Fn1* encoding fibronectin, was examined. The marker proteins are major precursors of matrix proteins in both normal and fibrotic lungs. The mRNA expression of *Col1a1*, *Col1a2*, and *Fn1* in the lungs was increased by MWCNT, which was statistically significant on day 3 and day 7 post-exposure to MWCNT (Fig. 2a). The protein levels of collagen I and fibronectin were dramatically increased in fibrotic lungs from mice exposed to MWCNT as shown by immunohistochemistry (Fig. 2b). Elevated expression of the proteins was mostly apparent in the interstitial fibrotic foci where MWCNT deposited. These data indicate induction of the fibrotic genes was directly involved in the progression of lung fibrosis induced by MWCNT.

## Prominent acute inflammation in mouse lungs exposed to MWCNT

A rapid increase of interstitial cellularity in MWCNT-exposed lungs suggests acute inflammation. Granulocytes, especially neutrophils, are among the first line of cells recruited to the site of inflammation to defend against foreign objects (microbes or particulates) and promote tissue recovery during acute inflammation. The cells of granulocytic lineage were visualized with the naphthol AS-D chloroacetate esterase reaction that specifically stains the granules of neutrophils, eosinophils, and basophils in lung

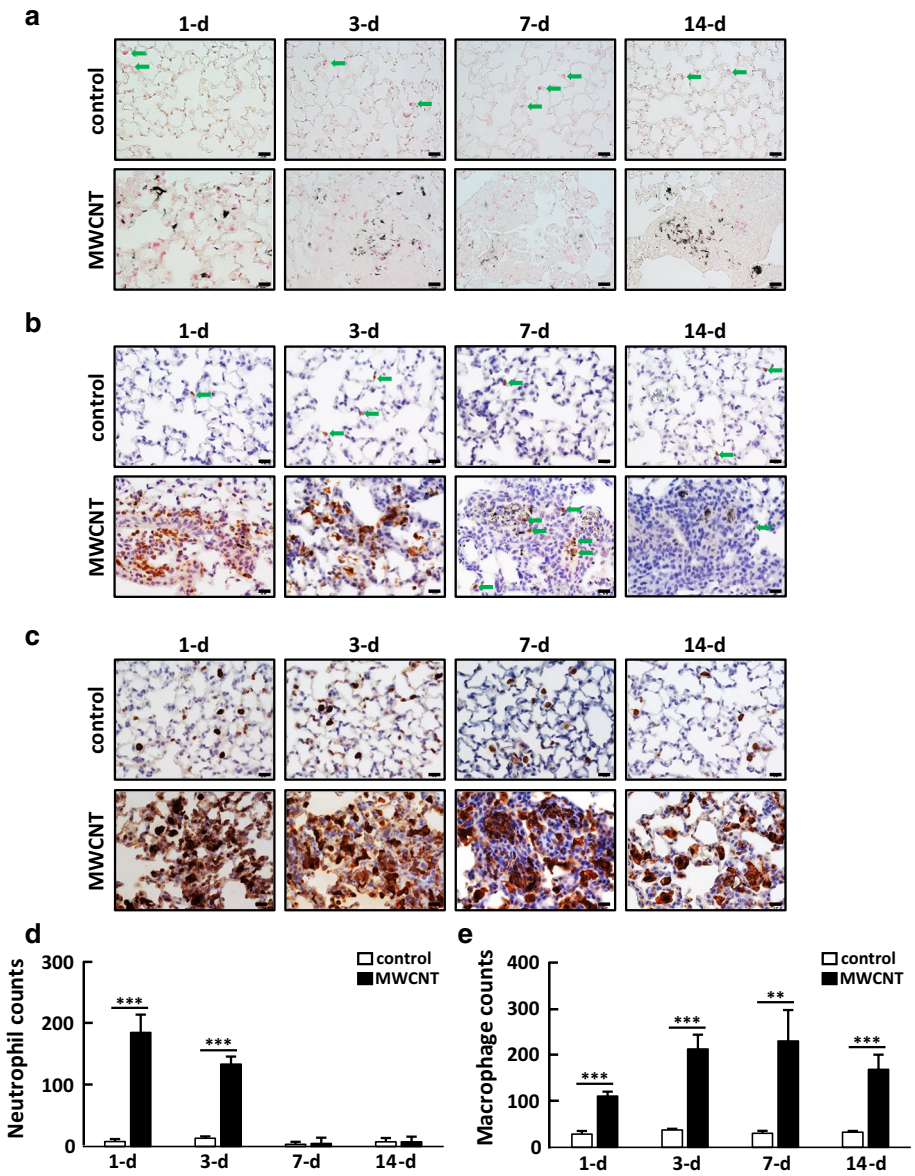


**Fig. 3** Inflammatory infiltration. Mice were treated with DM or MWCNT (40 μg). **a** Granulocytes. Paraffin-embedded lung sections were stained for Naphthol AS-D chloroacetate esterase activity. Esterase-positive granulocytes were indicated by *arrows* on control samples (*bright red*, *scale bar* 20 μm). **b** Neutrophils. Ly-6G and Ly-6C-positive neutrophils were detected by immunohistochemistry on lung sections (*red*, *scale bar* 20 μm). Nuclei were counterstained (*blue*). On the images with a limited number of neutrophils, neutrophils were indicated by *arrows*. **c** Macrophages. Mac-2-positive macrophages were detected by immunohistochemistry on lung sections (*red*, *scale bar* 20 μm). Nuclei were counterstained (*blue*). Quantification was shown for neutrophil infiltration **d** and macrophage infiltration **e**. Cell numbers were counted on five separate images taken under ×40 magnification for each lung tissue sample. Lung tissues from four mice per group were analyzed. Data were presented as mean ± SD

sections. Pulmonary exposure to MWCNT increased the number of granulocytes in the lung interstitial parenchyma dramatically on day 1 and day 3 post-exposure (Fig. 3a). Infiltration was reduced but remained at a significantly higher level than vehicle control on days 7 and 14. Infiltration was most significant at regions where pathologic foci and MWCNT deposits were found. Because neutrophils account for a majority of the granulocytes in most acute inflammation, we examined neutrophil infiltration by immunohistochemistry with antibodies against neutrophil marker proteins Ly-6G and Ly-6C. Neutrophil infiltration was dramatically increased on day 1 and day 3 post-exposure to MWCNT, but was decreased significantly on day 7 and day 14, which correlates with the time course of granulocyte infiltration qualitatively (Fig. 3b, d). Immunohistochemistry using antibodies against specific markers of eosinophils or basophils did not detect significant increase of either cell type at the early time points examined (data not shown). The results reveal that the early phase response includes an acute inflammatory course in which neutrophils dominate the early inflammatory infiltration.

Macrophages are another major type of cells with multiple roles in lung inflammation and fibrosis. We examined the increase of macrophages by immunohistochemistry using antibodies specific for the Mac-2 marker protein abundantly expressed on the surface of activated macrophages. Treatment with DM did not change the number of resident macrophages, but exposure to MWCNT significantly increased the number of Mac-2 positive macrophages in the lungs (Fig. 3c, e). Macrophage infiltration was observed in both the interstitial and alveolar spaces, but the interstitial fibrotic foci were the major sites of

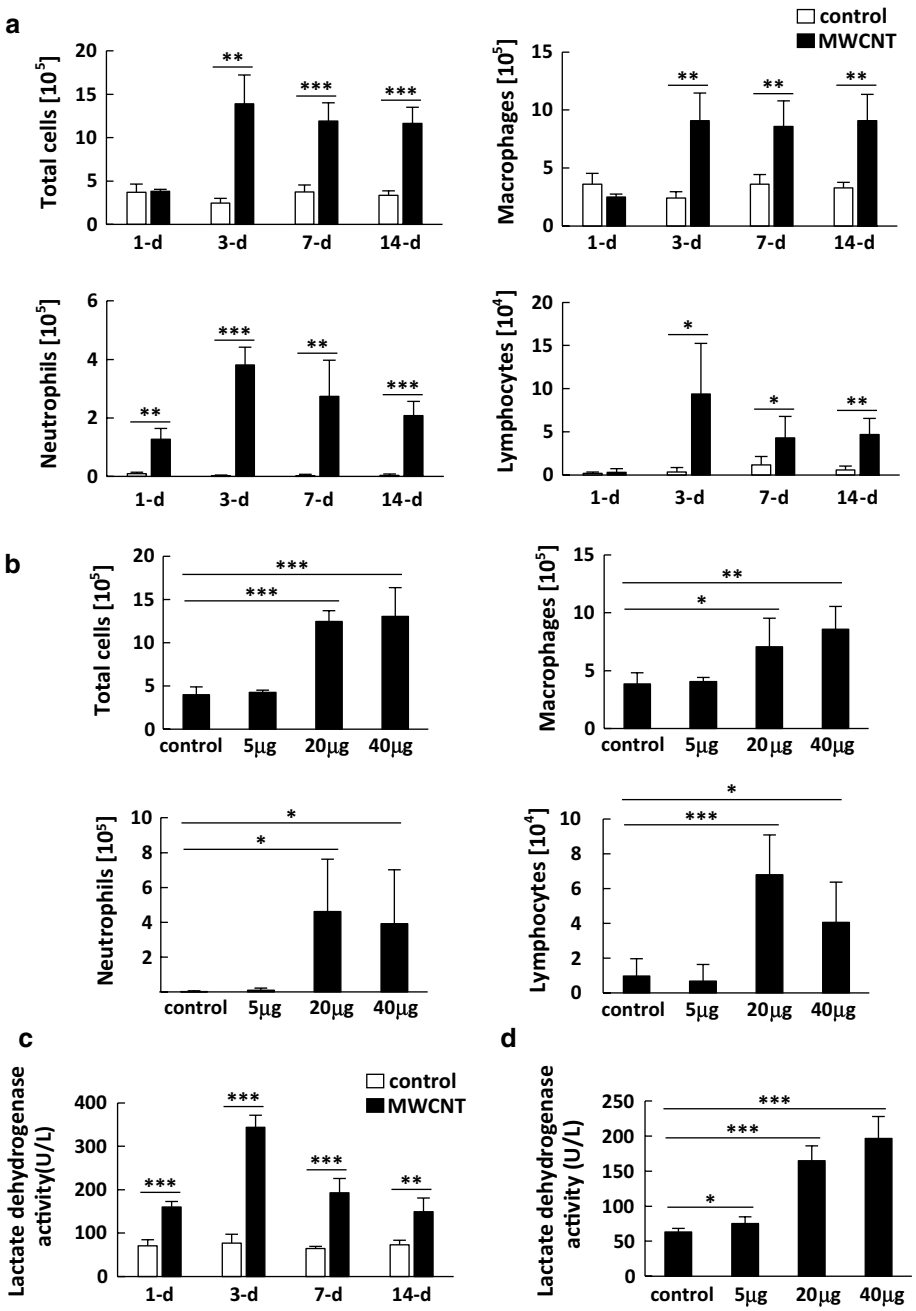


**Fig. 4** BAL fluid analysis. **a** Time course analysis of BAL cells. Counts of total cells, macrophages, neutrophils, and lymphocytes were analyzed in BAL fluid isolated from DM or 40 μg MWCNT-treated mice (mean ± SD, $n = 5$ for each group). **b** Dose-dependence analysis of BAL cells. Counts of total cells, macrophages, neutrophils, and lymphocytes were analyzed in BAL fluid from mice on day 7 post-exposure to a single dose of DM or MWCNT (mean ± SD, $n = 6$ for each group). BAL fluid LDH activities were shown for the time course study (**c**) or dose-dependence study (**d**)

macrophage accumulation. The increase was significant as early as day 1 post-exposure and continued till day 7, after which time, infiltration was reduced but remained significantly higher than control through day 14.

The BAL fluid from inflamed lungs contains inflammatory cells and proteins that reflect the inflammatory and injury status of the lung parenchyma. A time course analysis of the BAL fluid from mice treated with MWCNT showed that MWCNT induced a rapid increase in the number of neutrophils in BAL fluid on day 1 post-exposure (Fig. 4a). Neutrophils in BAL fluid continued to increase on day 3 followed by reduction on day 7 and day 14. Significant increases in the numbers of total cells, macrophages, and lymphocytes were observed on day 3 through day 14 post-exposure to MWCNT. The BAL fluid LDH activity is an indicator of injury in the lungs and was found significantly elevated on day 1 after MWCNT treatment (Fig. 4c). The LDH activity continued to increase on day 3, but diminished on days 7 and 14 with a time course similar to that of BAL neutrophil infiltration.

Exposure of mice to increasing doses of MWCNT significantly increased the numbers of total cells, neutrophils, macrophages, and lymphocytes at a dose of 20 or

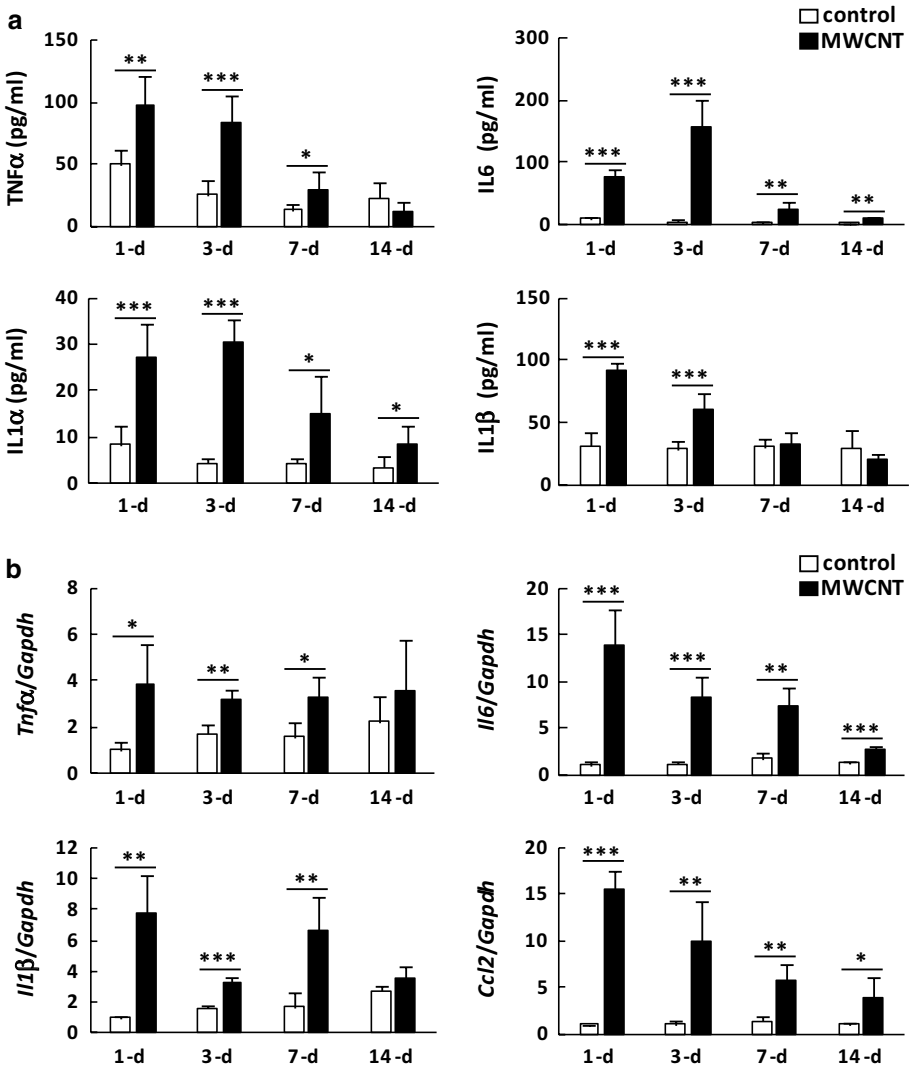


**Fig. 5** Induction of cytokine expression. **a** BAL fluid analysis. TNFα, IL6, IL1α, and IL1β levels in BAL fluid from mice treated with DM or MWCNT (40 μg) were determined using ELISAs (mean ± SD, $n = 6$ for each group). **b** mRNA expression in the lungs. Total RNA samples were isolated from lung tissues of mice exposed to DM or MWCNT (40 μg), and quantitative PCR was performed to determine the relative mRNA levels of inflammatory cytokine genes. Fold changes relative to *Gapdh* were calculated and expressed as mean ± SD ($n = 4$ for each group)

40 μg MWCNT (Fig. 4b). The LDH activity showed a dose-dependent increase in response to MWCNT exposure starting at 5 μg per mouse (Fig. 4d). These results on BAL fluid further confirm that MWCNT induced acute inflammation and tissue injury in the lungs. In aggregate, these analyses demonstrate that pulmonary exposure to MWCNT with a single treatment in the dose range of 5–40 μg per mouse elicited an acute inflammatory response in mouse lungs characterized by rapid infiltration of neutrophils and macrophages.

## Elevated expression of proinflammatory and profibrotic cytokines and growth factors

Upon recruitment by fibrogenic agents, inflammatory cells, examplified by macrophages, secrete multiple soluble factors including chemokines, cytokines, and growth factors to modulate inflammation and fibrosis in a context- and time-dependent manner. We have previously found that treatment of macrophages with MWCNT resulted in a conditioned medium that was capable of stimulating fibroblasts to transform into myofibroblasts, a key cellular event in lung fibrosis (He et al. 2011). The findings imply that a soluble factor(s) released from MWCNT-activated macrophages into the medium was responsible for the profibrotic cell transformation. To gain further insights into the underlying molecular mechanism of MWCNT-induced lung fibrosis, we analyzed the expression of a panel of proinflammatory and profibrotic cytokines and growth factors in mouse lungs exposed to MWCNT.

We first examined the protein levels of TNFα, IL6, IL1α, and IL1β in BAL fluid that represent secreted cytokines during acute lung inflammation. The proinflammatory cytokines in BAL fluid were markedly increased and reached a peak on day 1 for TNFα and IL1β, or day 3 for IL6 and IL1α, followed by reduction on day 7 and day 14, post-exposure to MWCNT (Fig. 5a). The dramatic increase followed by a rapid decrease of the cytokines likely reflects

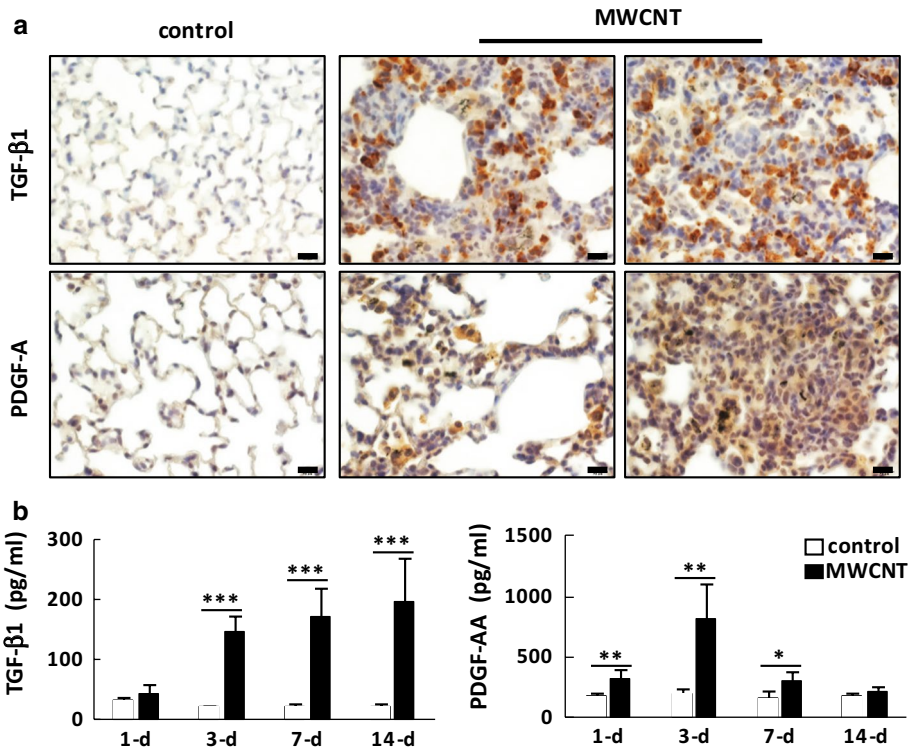


**Fig. 6** Increased expression of TGF and PDGF proteins in the lungs. **a** TGF-β1 and PDGF-A levels were assessed by immunohistochemistry of lung tissues from DM or 40 μg MWCNT-treated mice on day 7 after administration. *Red* indicates positive staining, and *blue* indicates nuclear staining (*scale bar* 20 μm). **b** Protein levels of TGF-β1 and PDGF-AA in BAL fluid from DM or 40 μg MWCNT-treated mice were determined using ELISAs (mean ± SD, $n = 5$ for each group)

the acute inflammatory course from which the cytokines were produced. The mRNA levels of TNFα, IL6, IL1β, and CCL2 in lung tissues were significantly elevated on day 1 after MWCNT treatment, and remained significantly higher than control through day 7 (TNFα, IL1β) or day 14 (IL6, CCL2), though a time-dependent reduction was noted for all cytokines (Fig. 5b). These data support the notion that MWCNT induced an acute inflammatory response in mouse lungs to result in elevated expression of proinflammatory and profibrotic cytokines that stimulate the initiation of lung fibrosis.

TGF-β1 and PDGF-A are growth factors secreted by macrophages and other lung cells and bind to their receptors on the surface of target cells, such as fibroblasts, to regulate cell proliferation and differentiation during fibrosis (Blobe et al. 2000; Trojanowska 2008). TGF-β1 and PDGF-A protein levels were dramatically increased in fibrotic lungs following treatment with MWCNT as shown by immunohistochemistry staining (Fig. 6a). Notably, the expression of TGF-β1 and PDGF-A was significantly higher in regions where fibrosis was taking place or had been well developed (Fig. 6a). Significantly, elevated levels of TGF-β1 and PDGF-AA (dimer of PDGF-A) in BAL fluid were observed on days 3, 7, and 14 post-exposure to MWCNT for TGF-β1, or on days 1, 3, and 7 for PDGF-AA (Fig. 6b). The peak level for TGF-β1 was on day 14 and that for PDGF-AA on day 3.

These data clearly demonstrate that pulmonary exposure to MWCNT markedly induced the expression and secretion of acute inflammatory cytokines and growth factors in both the lung parenchyma and BAL fluid, providing a molecular mechanism by which MWCNT induce the early phase lung fibrosis.

## Discussion

There is a growing interest in the pulmonary toxicity of carbon nanomaterials in recent years, because of the rapid increase in the production and commercialization of the materials, as well as their unique properties including respirable size, fiber-like shape, and remarkable biopersistence, attributes known to cause fibrosis in the lungs by fibrogenic fibers, such as asbestos (Donaldson et al. 2006; NIOSH 2013). A number of studies have shown that some forms of CNT are fibrogenic, inducing lung fibrosis in experimental animals upon pulmonary exposure (He et al. 2011, 2012; Porter et al. 2010; Shvedova et al. 2005). Moreover, the lung response to SWCNT or MWCNT exposure appears similar, including an acute phase response, marked by tissue injury and acute inflammation, and subsequent stable or progressive interstitial fibrosis, even though the CNT fibers differ considerably in their physical, chemical, and electronic properties (Mercer et al. 2011, 2013a). These observations imply that a common mechanism(s) exists and rules the pulmonary fibrotic response to CNT. However, little is known about how CNT

trigger and propagate lung fibrosis. Detailed analyses of the lung response to CNT at pathologic, cellular, and molecular levels are much needed to address this issue.

In this study, we focused on analyzing the pathologic and molecular features of the early phase response to pulmonary exposure of single-dose MWCNT. Quantitative and time course analyses uncovered that MWCNT induced rapid and marked fibrosis in the lungs, as early as day 1 after exposure to a low dose. The early fibrotic response was concomitant with pronounced pulmonary infiltration of inflammatory cells and elevated expression of fibrotic genes and proinflammatory/profibrogenic cytokines and growth factors. The findings reveal a new mechanistic aspect of CNT-induced lung fibrosis, wherein the interplay between acute inflammation and the early phase fibrotic response promotes the initiation and development of lung fibrosis through fibrogenic cells and mediators.

The functions of inflammatory cells and mediators in lung fibrosis are complex and in some cases controversial (Wynn 2011). The lung macrophages are likely to play a critical role in MWCNT-induced fibrosis, because a major portion of the MWCNT deposited in the lungs is within the macrophage compartment (Mercer et al. 2011). This unique distribution may account for their distinct kinetics in the lungs and greater tendency to induce interstitial granulomas at the chronic stage, compared with SWCNT. Importantly, MWCNT-activated macrophages may secret multiple soluble factors that regulate inflammation, matrix remodeling, and fibroblast functions. We previously found that a conditioned medium from MWCNT-treated macrophages evoked the transformation of fibroblasts to myofibroblasts, indicating a soluble factor(s) released from the macrophages activated the fibroblasts (He et al. 2011). This notion is strongly supported by our current finding that MWCNT induce the expression of a panel of proinflammatory and profibrotic cytokines and growth factors in the lungs.

MWCNT increased the protein levels of TNFα, IL1α, IL1β, and IL6 in the BAL fluid and the mRNA levels of TNFα, IL1β, IL6, and CCL2 in lung tissues. Cytokines reached peak levels within 1 or 3 days after treatment indicating an acute course. Among the cytokines, TNFα, IL6, IL1α, and IL1β are major proinflammatory cytokines in acute inflammation and are implicated in several fibrotic lung diseases in humans and animal models (Fielding et al. 2014; Hasegawa et al. 1997; Kolb et al. 2001; Lesur et al. 1994; Miyazaki et al. 1995; Suwara et al. 2014; Zhang et al. 1993). CCL2 is a member of the CC chemokine family that recruits macrophages and boosts collagen production during lung fibrosis (Gharaee-Kermani et al. 1996). The functional roles and mechanisms of regulation of the cytokines in MWCNT-induced lung fibrosis are to be examined in more details in future experiments. The rapid and dramatic induction of the cytokines by MWCNT suggests that these induced genes potentially serve as biomarkers of exposure and toxicity of CNT in humans.

A major finding of the study is the rapid onset of lung fibrosis, detected as early as day 1 after exposure to MWCNT. Concomitant to acute fibrosis, there was a rapid and significant induction of TGF-β1 and PDGF, two major fibrogenic factors, in the lungs, most apparently within the fibroblast foci and fibrotic septa. TGF-β1 has been well studied and is regarded as a principal fibrogenic mediator in a number of lung fibrosis models (Wynn 2011). TGF-β1 induces the recruitment of macrophages and fibroblasts and promotes fibroblast proliferation, which is possibly mediated through PDGF. TGF-β1 upregulates the expression of PDGF, thus further functioning in fibrosis. Both TGF-β1 and PDGF have been shown to drive the transformation of fibroblasts to myofibroblasts, a determining step in the process of fibrosis (Bonner 2004; Desmouliere et al. 1993; Trojanowska 2008). Together these observations suggest that TGF-β1 and PDGF play a major role in the acute fibrotic response to pulmonary exposure of MWCNT.

A variety of fibrogenic agents induce lung fibrosis in humans and animal models, including particles and fibers, such as asbestos and silica; lung toxicants, such as the anticancer drug bleomycin and herbicide paraquat; and organic dusts, such as moldy hay (Bus and Gibson 1984; Castranova and Vallyathan 2000; Dales and Munt 1982; Mouratis and Aidinis 2011; O'Reilly et al. 2007). An acute response is commonly observed in these cases of induced lung fibrosis. Presumably, exposure to fibrotic inducers causes damages to the pulmonary airways and parenchyma and, thereby, evokes inflammation and tissue repair that ultimately result in fibrosis in the lungs. Among the inducers, bleomycin and paraquat, administered either locally or systemically, accumulate in the lung epithelial cells and cause cell death by inducing DNA strand breaks or by reactive oxygen species-mediated cytotoxicity, respectively (Bus and Gibson 1984; Moore and Hogaboam 2008). In these scenarios, the acute response to the lung toxicants manifests extensive tissue damage and sometimes hemorrhage blended with acute inflammation. The asbestos fibers and silica particles inhaled into the lungs are phagocytized by macrophages to result in "frustrated phagocytosis", wherein macrophages are unable to get rid of the materials, but instead produce and release large quantities of cytotoxic agents to cause injury to local structures (Castranova and Vallyathan 2000). As a result, the acute response to inhaled fibers and particles is often marked by localized tissue damage and inflammation near where fibers and particles deposit, such as the first alveolar duct bifurcation and the interstitial space of alveolar septa (Brody and Roe 1983; Mercer et al. 2013a). Organic dusts induce hypersensitivity pneumonitis through type III and type IV reactions characterized by loosely formed interstitial granulomas and

inflammation (Dales and Munt 1982). In all cases, inflammation is a common component of the acute pulmonary response to the inducers. Whether these inducers elicit a marked fibrotic response in the acute phase similarly to the fibrotic response to CNT has not yet been addressed; and what role, if any, inflammation plays in inducing lung fibrosis by the inducers has remained controversial. From this prospect, our analyses of the acute fibrotic and inflammatory responses to MWCNT have generated new insights into these questions, which would facilitate future studies of induced lung fibrosis in humans.

In conclusion, single exposure to MWCNT at a low dose by pharyngeal aspiration induced rapid onset of fibrosis in mouse lungs with a detectable phenotype at day 1 and most dramatic phenotype at day 7 post-exposure. Fibrosis was characterized by increased deposition of collagen fibers in the alveolar septa and formation of fibrotic foci in the lung interstitial parenchyma, along with elevated expression of fibrotic genes. Fibrosis was accompanied by acute inflammation manifested as rapid infiltration of neutrophils and macrophages in lung tissues and the BAL fluid. Moreover, MWCNT induced elevated expression of a panel of proinflammatory cytokines TNFα, IL1α, IL1β, IL6, and CCL2, and fibrogenic growth factors TGF-β1 and PDGF-A in the lungs with distinct time courses. This study, for the first time, provided a detailed analysis of the early phase response to MWCNT. The findings reveal a molecular model in which the acute fibrotic and inflammatory responses interrelate through fibrogenic cells and factors to impact the initiation and propagation of interstitial fibrosis induced by MWCNT in mouse lungs.

**Acknowledgments** The study was supported by a grant to QM from National Institute for Occupational Safety and Health, Health Effects Laboratory Division. The anti-MBP antibody was kindly offered by Drs. Nancy A. Lee and James J. Lee at Mayo Clinic (Scottsdale, AZ, USA).

**Conflict of interest** The authors declare that they have no conflicts of interest.

**Ethical standard** All applicable international, national, and/or institutional guidelines for the care and use of animals were followed. All procedures performed in studies involving animals were in accordance with the ethical standards of the institution or practice at which the studies were conducted.

## References

Blobe GC, Schiemann WP, Lodish HF (2000) Role of transforming growth factor beta in human disease. N Engl J Med 342(18):1350–1358. doi:10.1056/NEJM200005043421807

Bonner JC (2004) Regulation of PDGF and its receptors in fibrotic diseases. Cytokine Growth Factor Rev 15(4):255–273. doi:10.1016/j.cytogfr.2004.03.006

Brody AR, Roe MW (1983) Deposition pattern of inorganic particles at the alveolar level in the lungs of rats and mice. Am Rev Respir Dis 128(4):724–729

Bus JS, Gibson JE (1984) Paraquat: model for oxidant-initiated toxicity. Environ Health Perspect 55:37–46

Buzea C, Pacheco II, Robbie K (2007) Nanomaterials and nanoparticles: sources and toxicity. Biointerphases 2(4):MR17–MR71

Castranova V, Vallyathan V (2000) Silicosis and coal workers' pneumoconiosis. Environ Health Perspect 108(Suppl 4):675–684

Dales RE, Munt PW (1982) Farmer's lung disease. Can Fam Physician Med 28:1817–1820

De Volder MF, Tawfick SH, Baughman RH, Hart AJ (2013) Carbon nanotubes: present and future commercial applications. Science 339(6119):535–539. doi:10.1126/science.1222453

Desmouliere A, Geinoz A, Gabbiani F, Gabbiani G (1993) Transforming growth factor-beta 1 induces alpha-smooth muscle actin expression in granulation tissue myofibroblasts and in quiescent and growing cultured fibroblasts. J cell biol 122(1):103–111

Donaldson K, Aitken R, Tran L et al (2006) Carbon nanotubes: a review of their properties in relation to pulmonary toxicology and workplace safety. Toxicol Sci 92(1):5–22. doi:10.1093/toxsci/kfj130

Fielding CA, Jones GW, McLoughlin RM et al (2014) Interleukin-6 signaling drives fibrosis in unresolved inflammation. Immunity 40(1):40–50. doi:10.1016/j.immuni.2013.10.022

Gharaee-Kermani M, Denholm EM, Phan SH (1996) Costimulation of fibroblast collagen and transforming growth factor beta1 gene expression by monocyte chemoattractant protein-1 via specific receptors. J Biol Chem 271(30):17779–17784

Hasegawa M, Fujimoto M, Kikuchi K, Takehara K (1997) Elevated serum tumor necrosis factor-alpha levels in patients with systemic sclerosis: association with pulmonary fibrosis. J Rheumatol 24(4):663–665

He X, Young SH, Schwegler-Berry D, Chisholm WP, Fernback JE, Ma Q (2011) Multiwalled carbon nanotubes induce a fibrogenic response by stimulating reactive oxygen species production, activating NF-kappaB signaling, and promoting fibroblast-to-myofibroblast transformation. Chem Res Toxicol 24(12):2237–2248. doi:10.1021/tx200351d

He X, Young SH, Ferback JE, Ma Q (2012) Single-walled carbon nanotubes induce fibrogenic effect by disturbing mitochondrial oxidative stress and activating NF-κB signaling. J Clin Toxicol S5:005. doi:10.4172/2161-0495.S5-005

Hubner RH, Gitter W, El Mokhtari NE, et al. (2008) Standardized quantification of pulmonary fibrosis in histological samples. Biotechniques 44(4):507–511, 514–517. doi:10.2144/000112729

Kolb M, Margetts PJ, Anthony DC, Pitossi F, Gauldie J (2001) Transient expression of IL-1beta induces acute lung injury and chronic repair leading to pulmonary fibrosis. J Clin Invest 107(12):1529–1536. doi:10.1172/JCI12568

Lesur OJ, Mancini NM, Humbert JC, Chabot F, Polu JM (1994) Interleukin-6, interferon-gamma, and phospholipid levels in the alveolar lining fluid of human lungs. Profiles in coal worker's pneumoconiosis and idiopathic pulmonary fibrosis. Chest 106(2):407–413

Maynard AM, Kuempel ED (2005) Airborne nanostructured particles and occupational health. J Nanopart Res 7:587–614

Mercer RR, Hubbs AF, Scabilloni JF et al (2010) Distribution and persistence of pleural penetrations by multi-walled carbon nanotubes. Part Fibre Toxicol 7:28. doi:10.1186/1743-8977-7-28

Mercer RR, Hubbs AF, Scabilloni JF et al (2011) Pulmonary fibrotic response to aspiration of multi-walled carbon nanotubes. Part Fibre Toxicol 8:21. doi:10.1186/1743-8977-8-21

Mercer RR, Scabilloni JF, Hubbs AF et al (2013a) Distribution and fibrotic response following inhalation exposure to multi-walled carbon nanotubes. Part Fibre Toxicol 10(1):33. doi:10.1186/1743-8977-10-33

Mercer RR, Scabilloni JF, Hubbs AF et al (2013b) Extrapulmonary transport of MWCNT following inhalation exposure. Part Fibre Toxicol 10(1):38. doi:10.1186/1743-8977-10-38

Miyazaki Y, Araki K, Vesin C et al (1995) Expression of a tumor necrosis factor-alpha transgene in murine lung causes lymphocytic and fibrosing alveolitis. A mouse model of progressive pulmonary fibrosis. J Clin Invest 96(1):250–259. doi:10.1172/JCI118029

Moore BB, Hogaboam CM (2008) Murine models of pulmonary fibrosis. Am J Physiol Lung Cell Mol Physiol 294(2):L152–L160. doi:10.1152/ajplung.00313.2007

Mouratis MA, Aidinis V (2011) Modeling pulmonary fibrosis with bleomycin. Curr Opin Pulm Med 17(5):355–361. doi:10.1097/MCP.0b013e328349ac2b

NIOSH (2013) Current strategies for engineering controls in nanomaterial production and downstream handling processes, vol HDDS (NIOSH) Publication No. 2014-102. Department of Health and Human Services, Centers for Disease Control and Prevention, National Institute for Occupational Safety and Health, Cincinnati

O'Reilly KM, McLaughlin AM, Beckett WS, Sime PJ (2007) Asbestos-related lung disease. Am Fam Physician 75(5):683–688

Porter DW, Sriram K, Wolfarth MG et al (2008) A biocompatible medium for nanoparticle dispersion. Nanotoxicology 2:144–154

Porter DW, Hubbs AF, Mercer RR et al (2010) Mouse pulmonary dose- and time course-responses induced by exposure to multi-walled carbon nanotubes. Toxicology 269(2–3):136–147. doi:10.1016/j.tox.2009.10.017

Porter DW, Hubbs AF, Chen BT et al (2013) Acute pulmonary dose-responses to inhaled multi-walled carbon nanotubes. Nanotoxicology 7(7):1179–1194. doi:10.3109/17435390.2012.719649

Rao GV, Tinkle S, Weissman DN et al (2003) Efficacy of a technique for exposing the mouse lung to particles aspirated from the pharynx. J Toxicol Environ Health Part A 66(15):1441–1452. doi:10.1080/15287390306417

Rom WN (2007) Environmental and occupational medicine, 4th edn. Lippincott Williams and Wilkins, Philadelphia

Ryman-Rasmussen JP, Cesta MF, Brody AR et al (2009) Inhaled carbon nanotubes reach the subpleural tissue in mice. Nat Nanotechnol 4(11):747–751. doi:10.1038/nnano.2009.305

Shvedova AA, Kisin ER, Mercer R et al (2005) Unusual inflammatory and fibrogenic pulmonary responses to single-walled carbon nanotubes in mice. Am J Physiol Lung Cell Mol Physiol 289(5):L698–L708. doi:10.1152/ajplung.00084.2005

Suwara MI, Green NJ, Borthwick LA et al (2014) IL-1alpha released from damaged epithelial cells is sufficient and essential to trigger inflammatory responses in human lung fibroblasts. Mucosal Immunol 7(3):684–693. doi:10.1038/mi.2013.87

Trojanowska M (2008) Role of PDGF in fibrotic diseases and systemic sclerosis. Rheumatology 47(Suppl 5):v2–v4. doi:10.1093/rheumatology/ken265

Wynn TA (2011) Integrating mechanisms of pulmonary fibrosis. J Exp Med 208(7):1339–1350. doi:10.1084/jem.20110551

Zhang Y, Lee TC, Guillemin B, Yu MC, Rom WN (1993) Enhanced IL-1 beta and tumor necrosis factor-alpha release and messenger RNA expression in macrophages from idiopathic pulmonary fibrosis or after asbestos exposure. J Immunol 150(9):4188–4196

Zhang Q, Huang JQ, Qian WZ, Zhang YY, Wei F (2013) The road for nanomaterials industry: a review of carbon nanotube production, post-treatment, and bulk applications for composites and energy storage. Small 9(8):1237–1265. doi:10.1002/smll.201203252